IEEE Access
Multidisciplinary | Rapid Review | Open Access Journal

Received May 19, 2020, accepted June 22, 2020, date of publication July 6, 2020, date of current version July 17, 2020.

Digital Object Identifier 10.1109/ACCESS.2020.3007316

A 26GHz CMOS 3× Subharmonic Mixer With a Fundamental Frequency Rejection Technique

HYO-SUNG LEE[1], (Member, IEEE), JONGHOON MYEONG[2], (Graduate Student Member, IEEE), AND BYUNG-WOOK MIN[2], (Member, IEEE)

[1]Samsung Electronics, Suwon 16677, South Korea
[2]School of Electrical and Electronic Engineering, Yonsei University, Seoul 03722, South Korea

Corresponding author: Byung-Wook Min (bmin@yonsei.ac.kr)

This work was supported in part by the Yonsei-Samsung Strategy Research Center (YSSRC), and in part by the Institute of Information and Communications Technology Planning and Evaluation (IITP) grant funded by the Korea government (MSIT) under Grant 2020000218.

ABSTRACT A 26GHz up-conversion 3× sub-harmonic mixer is designed using a 65 nm CMOS process. The reasons for the lack of research on the 3× subharmonic mixer are investigated and a solution called a fundamental frequency rejection technique is presented. The fundamental frequency rejection technique allows the cancellation of the fundamental LO and boosting of the third-order harmonic. The proposed 3× subharmonic mixer consists of an octet-phase generator, 3× subharmonic mixer core, output transformer balun, and LO buffers. The octet-phase generator, which consists of a transformer balun and a two-stage polyphase filter, provides the 8-phase LO for the fundamental frequency rejection technique. The mixer core consists of three Gilbert-cell active sub-mixers to implement the fundamental frequency rejection technique. The measured conversion gain of the 3× subharmonic mixer is −5.1±1.5 dB at the RF of 19.5−31.5 GHz. The measured OP_{1dB} and OIP3 are −15.4 dBm and −7.6 dBm, respectively. The LO-RF isolation and 3LO-RF isolation are >42 dB and >46 dB, respectively, at the operating frequency. The proposed 3× subharmonic mixer consumes DC power of 55.65 mW and occupies a die area of 0.267 mm^2.

INDEX TERMS 3× subharmonic mixer, CMOS, fundamental frequency rejection technique, octet-phase generator, polyphase filter.

I. INTRODUCTION

The direct-conversion transceiver architecture has been commonly employed in wireless communication systems owing to its simple design with low power consumption and high integration compared with the heterodyne transceiver architecture [1], [2]. The direct-conversion transceiver does not require an intermediate frequency (IF) filter and an image rejection (IR) filter, which are usually designed as a discrete component at off-chip, owing to the zero IF. Therefore, the direct-conversion transceiver can achieve high integration and low cost. However, as the local oscillator (LO) frequency is equal to the center frequency of the radio frequency (RF) spectrum, serious problems such as self-mixing at the receiver and LO pulling at the transmitter occur [2], [3]. A subharmonic mixer (SHM), typically utilizing the second-order harmonic of the mixer, is a promising solution to self-mixing and LO pulling, because it can reduce the LO frequency to half the RF spectrum. In addition, thanks to the lower LO frequency, the phase noise performance and power consumption of the frequency synthesizer are improved [4]. Therefore, the subharmonic mixer is very attractive for high-frequency applications such as millimeter-wave because it is difficult to satisfy the required phase noise and power consumption with the high-frequency LO design [5]–[7].

Although significant research has been conducted on the second-order SHMs (2×SHMs), which reduce the LO frequency(f_{LO}) to half [8]–[13], the studies on the third-order SHMs (3×SHMs) [14], which reduce f_{LO} by one-third, have been scant. There are some reasons for this. Firstly, the third-order harmonic level of a general non-linear device is relatively lower than the second-order harmonic level. Secondly, a 3×SHM translates the baseband(BB) signal at f_{BB} not only to $3f_{LO} \pm f_{BB}$ tones, but also to $f_{LO} \pm f_{BB}$ tones, which are usually rejected in a 2×SHM with differential phases of LO signal. The $f_{LO} \pm f_{BB}$ tones can be converted to the third-order harmonics, $3f_{LO} \pm 3f_{BB}$ tones, at the non-linear device located after the 3×SHM. These tones locate within

The associate editor coordinating the review of this manuscript and approving it for publication was Dušan Grujić.

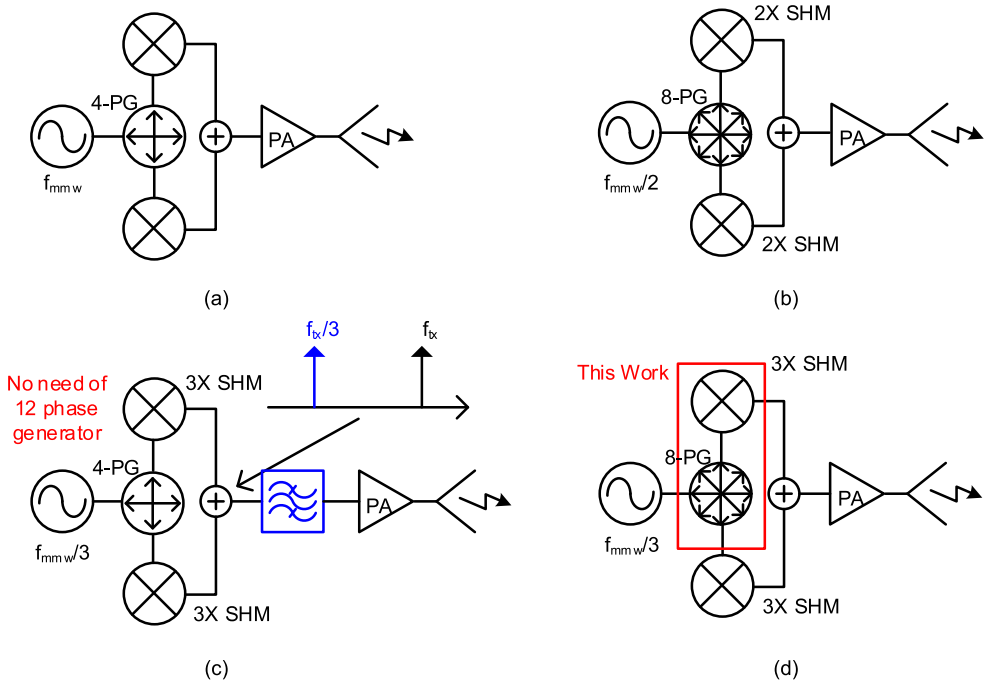

FIGURE 1. Block diagram of direct-conversion transmitters with (a) a LO mixer and 4-PG, (b) 2×SHMs and 8-PG, (c) 3×SHMs and 4-PG, and (d) 3×SHMs and 8-PG.

TABLE 1. Comparison table with Mixer types.

Mixer type	System	LO freq	LO phase step	Harmonics filter
Fund. mixer	Fig. 1(a)	f_{mmw}	90°(4 phases)	-
2× sub-mixer	Fig. 1(b)	1/2 f_{mmw}	45°(8 phases)	-
3× sub-mixer	-	1/3 f_{mmw}	30°(12 phases)	required
	Fig. 1(c)	1/3 f_{mmw}	90°(4 phases)	required
	Fig. 1(d) (this work)	1/3 f_{mmw}	45°(8 phases)	-

the intended transmitting spectrum around $3f_{LO} \pm f_{BB}$ and distort the transmitting signal. Therefore, the $f_{LO} \pm f_{BB}$ tones must be removed before the non-linear device, and a band-pass filter (BPF) is always necessary after the 3×SHM, which defeats the benefit of the direct-conversion architecture that requires no IF filter. To use 3×SHM in the direct-conversion transceiver, one should reject the fundamental tones within the 3×SHM without filter and extra burden on other circuits such as LO.

Fig. 1 and Table 1 show a block diagram of direct-conversion transmitters with the conventional mixer, 2×SHM, 3×SHM, and the proposed 3×SHM. As shown in Fig. 1(a), direct-conversion system with the same RF and LO frequency is an I/Q modulator using a 4-phase generator(PG), and even a 8-PG is required for the harmonic rejection mixer [15]. A direct-conversion transmitter with 2×SHM always requires 8-PG as shown in Fig. 1(b). It is easy to think that a 12-PG is required for a 3×SHM, but the 3×SHM can be implemented with the same 4-PG as in Fig.1(c) instead of a 12-PG with 30° intervals. The 4-PG can also generate the quadrature phase of $3f_{LO}$ since 0° and 90° LO signals can be considered as 0° and −90° LO signals at $3f_{LO}$ from $3\times90° = -90°$. Therefore, the 3×SHM system has an advantage over the 2× SHM system because it requires less LO phases. However, a BPF is required to remove unwanted signals at 1/3 frequency of the intended signal due to fundamental mixing. This BPF can be eliminated if a 8-PG is adopted in the 3×SHM system as in Fig. 1(d). Since the 8-PG is required even in the 2×SHM system and the harmonic reject mixer system, we can lower the LO frequency without generating more LO phases.

In the following section II, a new 3×SHM with fundamental frequency rejection technique for the elimination of a BPF is introduced. This can allow the full integration of the direct-conversion transmitter with 3×SHMs by eliminating the necessity of a BPF. A new 8-PG optimized for the fundamental frequency rejection technique is also introduced. the implemented 3×SHM is described and measured in the Section III and IV.

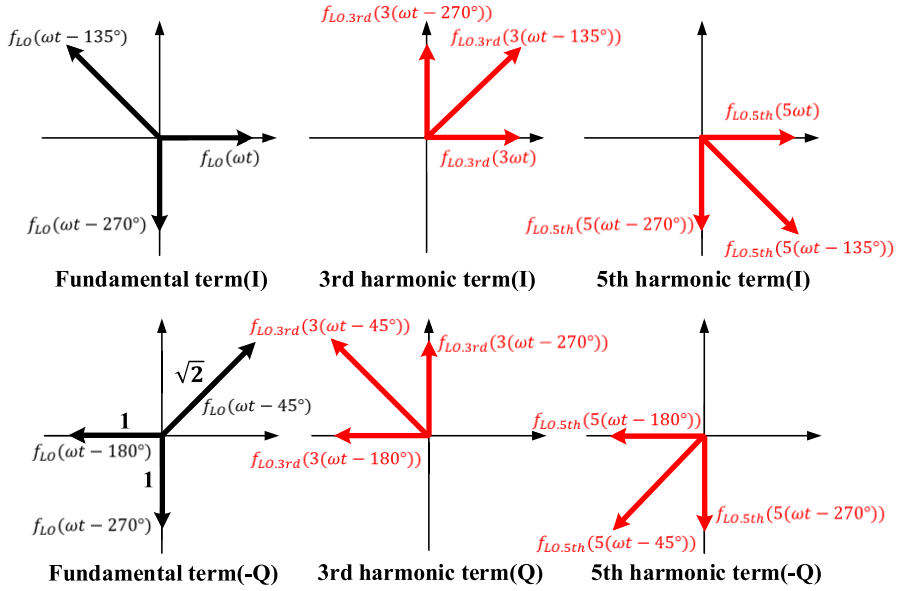

FIGURE 2. Vector diagram of fundamental frequency rejection technique.

II. CONCEPT OF A NEW 3× SUBHARMONIC MIXER

The concept of a new 3×SHM using fundamental frequency rejection technique can be easily explained by the vector diagram as shown in Fig. 2. The fundamental term (I) can be cancelled by combining three LO signals with the phases 0°, 90°, and 225°, at an amplitude ratio of 1:1:$\sqrt{2}$. The phases of the third-order harmonics of these LO signals are three times the phases of the fundamental LO signals and are 0°, −90°(270°), and −45°(675°), respectively (3rd harmonic term(I)). The amplitude of the final third-order harmonic is boosted to $2\sqrt{2}$ times compared with the use of a single LO signal. The fifth- order harmonic is also boosted $2\sqrt{2}$ times similarly. By using this technique, a 3×SHM and a 5x SHM can be designed.

The quadrature phase of the third-order harmonic can be generated by summing the three LO signals, as the fundamental term (-Q) in Fig. 2. Three LO signals, whose phases are 0°, 135°, and 270°, are combined at an amplitude ratio of 1:$\sqrt{2}$:1 and the phases of their third-order harmonics become 0°, 45°(405°), and 90°(810°), respectively. This 3rd harmonic term (Q) leads by 90° over the 3rd harmonic term (I). Therefore, an 8-phase LO is required to generate the differential-quadrature third-order harmonic LO in the direct-conversion transmitter with a new 3×SHM. Unlike the third-order harmonic, the fundamental term (-Q) generates the negative-quadrature fifth-order harmonic (5th harmonic term (-Q)). Therefore, the phase inversion of the fundamental term is required in the I/Q modulator with a 5x SHM.

The final LO waveform, $f_{LO.total}(\omega t)$, can be generated by summing the three fundamental LO waves. The three square waves whose phases are 0°, 90°, and 225° are summed at an amplitude ratio of 1:1:$\sqrt{2}$ to perfectly cancel the fundamental LO. Fundamental cancellation and third- and fifth-order harmonic boosting can be represented by a Fourier series. The expression for the final LO waveform, which is the sum of three fundamental LO signals, is given by

$$\begin{aligned} &f_{LO.total}(\omega t) \\ &= f_{LO}(\omega t) + f_{LO}(\omega t - \frac{\pi}{2}) + \sqrt{2} f_{LO}(\omega t - \frac{5}{4}\pi) \\ &\quad + 2\sqrt{2}A[\frac{1}{3}\sin(3\omega t + \frac{\pi}{4}) + \frac{1}{5}\sin(5\omega t - \frac{\pi}{4}) \ldots] \end{aligned} \quad (1)$$

The fundamental LO terms are eventually cancelled, whereas the amplitudes of the third- and fifth-order harmonics are boosted by $2\sqrt{2}$ times compared with the use of a single square wave. The general formula of the final LO waveform is as follows:

$$\begin{aligned} f_{LO.total}(\omega t) = 2\sqrt{2}A \sum_{n=1}^{\infty} [&\frac{1}{8n-5}\sin((8n-5)\omega t + \frac{\pi}{4}) \\ &+ \frac{1}{8n-3}\sin((8n-3)\omega t - \frac{\pi}{4})] \end{aligned} \quad (2)$$

The (8n-5)th-order and (8n-3)th-order harmonics increase by a factor of $2\sqrt{2}$. Further, the (8n-7)th-order harmonics and (8n-1)th-order harmonics are cancelled. As the ninth-order harmonic causing intermodulation distortion is rejected, the need for a BPF after the I/Q modulator is alleviated. The method of combining the three square waves has been studied extensively in the harmonic rejection mixer [15]. In this work, three fundamental LO signals are combined using a Gilbert-cell active mixer, one of the representative current-commutating mixers. Further details are presented in section IV-B.

Fig. 3 shows a direct-conversion transmitter with the proposed 3×SHM applying the fundamental frequency rejection technique. The octet-phase generator(8-PG) is

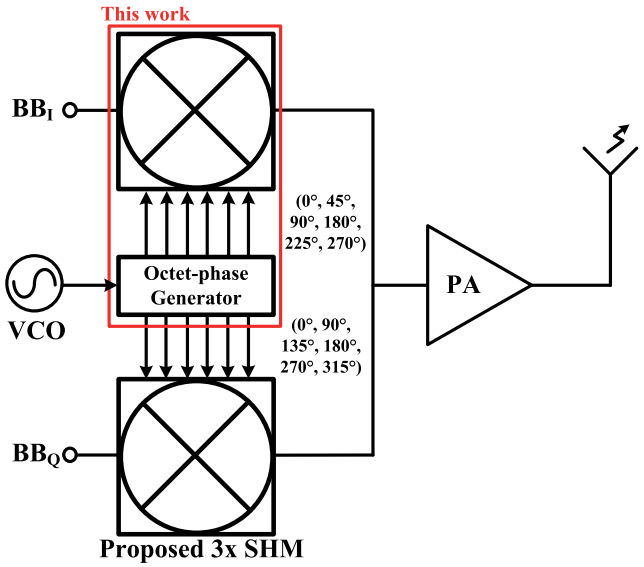

FIGURE 3. Direct-conversion transmitter with a proposed 3×SHM.

necessary to cancel the fundamental LO and produce balanced third-order harmonics of in-phase and quadrature phase. The BPF after the I/Q modulator is not employed because the new 3×SHM suppresses fundamental tones and ninth-order harmonics. This can allow the full integration of the direct-conversion transmitter. The required LO frequency is lowered to one-third of the transmitted frequency owing to the 3×SHM. LO pulling and power consumption performance are improved by decreasing the LO frequency to one-third. Hence, the direct-conversion transmitter using the proposed 3×SHM as shown in Fig. 3 is attractive in millimeter-wave communication systems. In this work, a prototype consisting of a new 3×SHM, 8-PG, transformer balun, and LO buffers is implemented using a 65 nm CMOS process. The details are described in the following section.

III. PROTOTYPE DESIGN AND IMPLEMENTATION

Fig. 4 shows a block diagram of a prototype of the new 3×SHM. To supply balanced LO signals to the 3×SHM, 6-phase LO signals whose phases are 0°, 180°, 225°, 45°, 90°, and 270° are required. However, the octet-phase generator generates an 8-phase LO signal with a phase interval of 45°. The remaining LO signals whose phases are 135° and 315° are connected to dummy buffers to alleviate a mismatch. LO buffers are employed to compensate the loss of an octet-phase generator. The LO buffer consists of a general 4-stage inverter type amplifier. The transformer balun at the output not only provides load inductance of the 3×SHM but also converts a balanced signal to an unbalanced signal. The transformer balun is designed and optimized with an electromagnetic simulator (Sonnet).

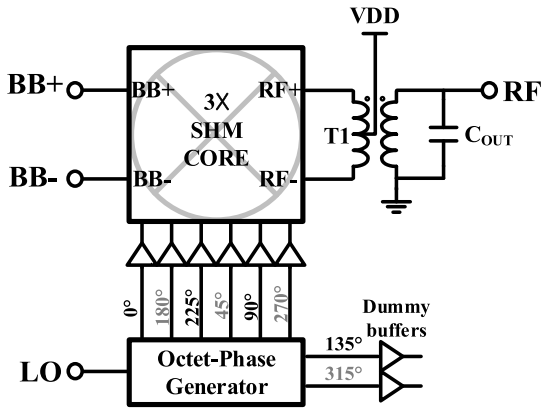

FIGURE 4. Block diagram of a prototype 3×SHM.

A. OCTET-PHASE GENERATOR

1) CONCEPT OF OCTET-PHASE GENERATOR

The octet-phase generator can be implemented with a 4-phase polyphase filter(PPF) and 45° phase shifting adders [8]. The 8-phase PPF in [11], [12] can also generate the octet-phase LO signals. In this work, the octet-phase LO signal is obtained from a two-stage 4-phase PPF. Fig. 5 shows a schematic of the proposed octet-phase generator. The octet-phase generator consists of a transformer balun and a two-stage PPF. The transformer balun converts a single-ended LO signal to a differential LO signal. The first PPF converts the differential LO signal to differential-quadrature LO signals. The amplitude scale of the four output signals is $\sqrt{2}/4$ (not $\sqrt{2}/2$) at the center frequency of PPF, when the second PPF is the same as the first PPF [16]. The second PPF converts the differential-quadrature LO signals to $\sqrt{2}$ times scaled and 45° phase-shifted differential-quadrature LO signals. The proposed octet-phase generator can generate an 8-phase LO signal using both the differential-quadrature LO signals and the 45° phase-shifted differential-quadrature LO signals. However, all the amplitudes of the octet-phase LO signals are not the same. The 45° phase-shifted differential-quadrature LO signals obtained after the second PPF are $\sqrt{2}$ times bigger than the other LO signals obtained after the first PPF. This octet-phase generator is suitable for the proposed 3×SHM because it requires 45° phase-shifted and $\sqrt{2}$ times differential-quadrature LO signals. This can allow for the perfect fundamental LO rejection and the third-order harmonic boosting as shown in Fig. 2. Since the transfer function of the

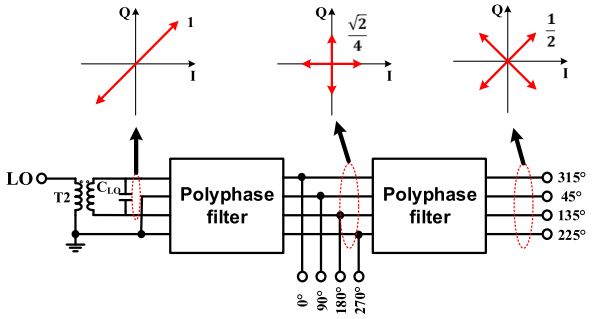

FIGURE 5. Proposed octet-phase generator and its vector response.

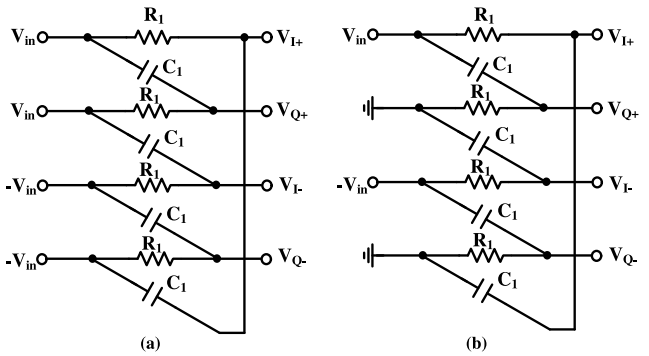

FIGURE 6. Quadrature generator with a single-stage PPF (a) two inputs connected, and (b) two inputs shorted to the ground.

mixer is nonlinear, scaling the transconductance(transistor size) rather than the amplitude scaling of the LO would be advantageous in terms of linearity.

2) QUADRATURE GENERATOR WITH A SINGLE-STAGE POLYPHASE FILTER

There are two ways to generate a differential-quadrature signal from a differential signal with a single-stage PPF as shown in Fig. 6. The differential-quadrature output of the two input-connected case shown in Fig. 6(a) is

$$V_{I\pm} = \pm V_{in}\left(\frac{1-j\omega R_1C_1}{1+j\omega R_1C_1}\right) = \pm V_{in}\left(\frac{1-j(\omega/\omega_0)}{1+j(\omega/\omega_0)}\right)$$
$$V_{Q\pm} = \pm V_{in} \tag{3}$$

where $\omega_0 = (R_1C_1)^{-1}$. The output I/Q signals maintain the same amplitudes at all frequencies as shown in Fig. 7(a). However, the quadrature difference of the I/Q signals increases away from the center frequency of the PPF.

The differential-quadrature output with two inputs shorted to the ground as shown in Fig. 6(b) is

$$V_{I\pm} = \pm V_{in}\left(\frac{1}{1+j\omega R_1C_1}\right) = \pm V_{in}\left(\frac{1}{1+j(\omega/\omega_0)}\right)$$
$$V_{Q\pm} = \pm V_{in}\left(\frac{j\omega R_1C_1}{1+j\omega R_1C_1}\right) = \pm V_{in}\left(\frac{j(\omega/\omega_0)}{1+j(\omega/\omega_0)}\right) \tag{4}$$

where $\omega_0 = (R_1C_1)^{-1}$. The output I/Q signals maintain a quadrature difference at all frequencies as shown in Fig. 7(b). However, the amplitude mismatch of I/Q signals increases away from the center frequency. Although the error function of the two quadrature generators is the same [17], the case with two inputs shorted to ground as shown in Fig. 6(b) is used in this work. The phase mismatch is a more serious problem than the amplitude mismatch in this 3×SHM.

3) TWO-STAGE POLYPHASE FILTER

Fig. 8 shows a schematic of a 2-stage PPF with two inputs shorted to the ground. As the proposed octet-phase generator uses both the first-stage output and the second-stage output signals, both should be analyzed. The differential-quadrature

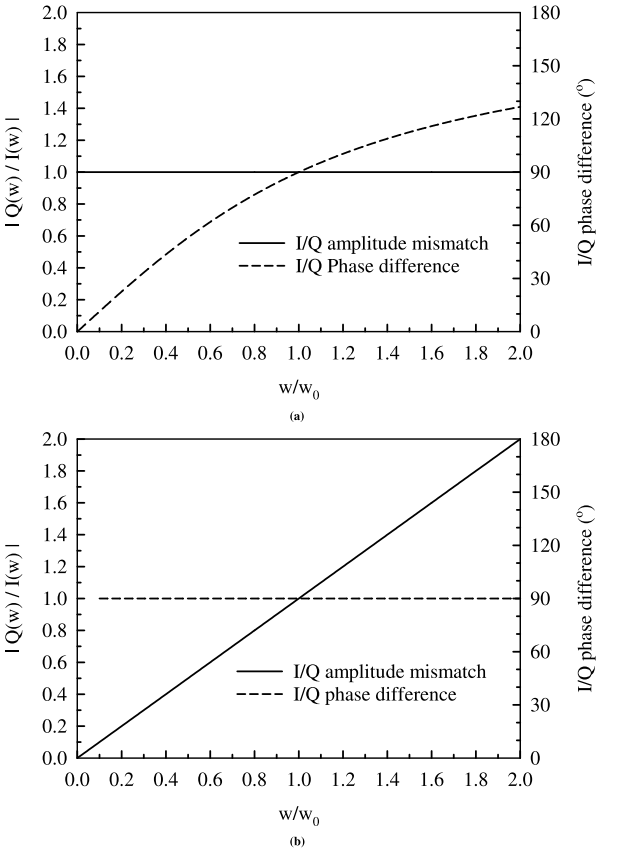

FIGURE 7. Output frequency response of quadrature output of a PPF. (a) two inputs connected, and (b) two inputs shorted to the ground.

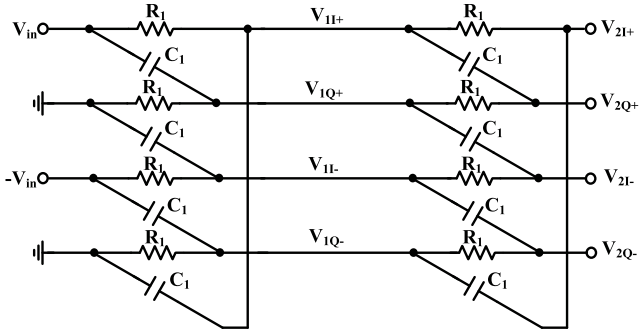

FIGURE 8. Schematic of the 2-stage polyphase filter with two inputs shorted to the ground.

output of the first stage is

$$V_{1I\pm} = \pm V_{in}\left(\frac{1+j(\omega/\omega_0)}{(1+j(\omega/\omega_0))^2+2j(\omega/\omega_0)}\right)$$
$$V_{1Q\pm} = \pm V_{in}\left(\frac{j(\omega/\omega_0)(1+j(\omega/\omega_0))}{(1+j(\omega/\omega_0))^2+2j(\omega/\omega_0)}\right) \tag{5}$$

and the differential-quadrature output of the second stage is

$$V_{2I\pm} = \pm V_{in}\left(\frac{1+(\omega/\omega_0)^2}{(1+j(\omega/\omega_0))^2+2j(\omega/\omega_0)}\right)$$
$$V_{2Q\pm} = \pm V_{in}\left(\frac{2j(\omega/\omega_0)}{(1+j(\omega/\omega_0))^2+2j(\omega/\omega_0)}\right) \tag{6}$$

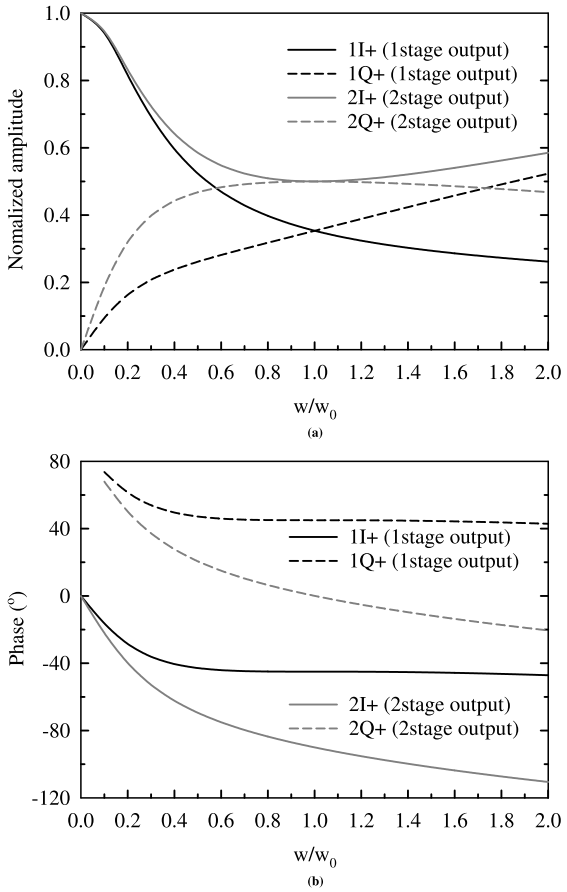

FIGURE 9. Normalized amplitude (a) and phase (b) of the 2-stage PPF outputs over the normalized frequency.

Equations (5) and (6) can be plotted as shown in Fig. 9. The I/Q signals in the first-stage output maintain a quadrature difference, but the amplitude mismatch increases away from the center frequency of the PPF. The I/Q mismatch ratio is the same as that shown in Fig. 6(b). The amplitudes of the second-stage output are $\sqrt{2}$ times as high as the first-stage output at $\omega = \omega_0$ (Fig. 9(a)). However, the amplitude mismatch also increases away from the center frequency of the PPF. The I/Q signals of both the first-stage output and second-stage output maintain a quadrature difference at all frequencies(Fig. 9(b)). The phases of the second-stage output are shifted by 45° than the phases of the first-stage output at $\omega = \omega_0$. The I/Q signals of the first-stage output have a large amplitude variation and a small phase variation, and the I/Q signals of the second-stage output have a small amplitude variation and a large phase variation.

The fundamental frequency rejection technique requires three-phase signals with 0°, 90°, and 225° phases at the amplitude ratio of 1:1:$\sqrt{2}$ as shown in Fig. 2. The 2-stage PPF as shown in Fig 8 can generate these signals. The sum of the three differential signals is expressed as follows:

$$\begin{aligned} V_{1I+} + V_{1Q-} + V_{2I-} &= 0 \\ V_{1I-} + V_{1Q+} + V_{2I+} &= 0 \end{aligned} \tag{7}$$

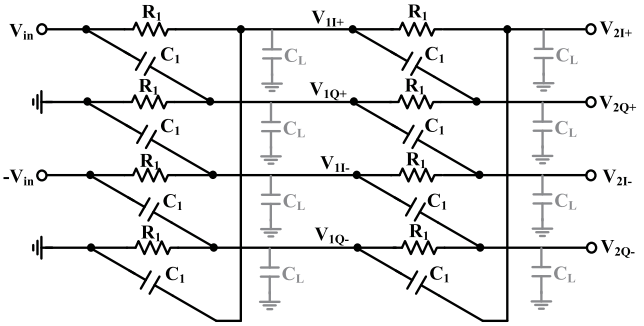

FIGURE 10. Schematic of an octet-phase generator with load capacitor.

The fundamental signal is perfectly cancelled regardless of the frequency. However, this 2-stage PPF is connected to LO buffers or switching cores of the mixer, which can be modeled as load capacitors. The following section analyzes the 2-stage PPF with load capacitors.

4) TWO-STAGE POLYPHASE FILTER WITH LOAD CAPACITORS

Fig. 10 shows the schematic of a 2-stage PPF with load capacitors. A load capacitor(C_L) is considered both the first-stage output and the second-stage output. The differential-quadrature output of the first stage is

$$\begin{aligned} V_{1I\pm} &= \pm V_{in}\left(\frac{1+j(\omega/\omega_0)(1+C_L/C_1)}{A(\omega)}\right) \\ V_{1Q\pm} &= \pm V_{in}\left(\frac{j(\omega/\omega_0)(1+j(\omega/\omega_0)(1+C_L/C_1))}{A(\omega)}\right) \end{aligned} \tag{8}$$

$$\begin{aligned} A(\omega) = {} & (1 + j(\omega/\omega_0)(1 + C_L/C_1))^2 \\ & + j(\omega/\omega_0)(1 + j(C_L/C_1)(\omega/\omega_0))(1 - j(\omega/\omega_0)) \\ & + j(\omega/\omega_0)(1 + C_L/C_1)(1 + j(\omega/\omega_0)) \end{aligned} \tag{9}$$

The load capacitors reduce the amplitudes and rotate the phases of the I/Q signals as shown in Fig 11. However, the I/Q mismatch ratio is the same as that shown in Fig. 6.(b). The differential-quadrature output of the second stage is

$$\begin{aligned} V_{2I\pm} &= \pm V_{in}\left(\frac{1+(\omega/\omega_0)^2}{A(\omega)}\right) \\ V_{2Q\pm} &= \pm V_{in}\left(\frac{2j(\omega/\omega_0)}{A(\omega)}\right) \end{aligned} \tag{10}$$

The load capacitors at the second stage also reduce the amplitudes and rotate the phases of the I/Q signals of the second-stage output. The phase difference between the first-stage output and the second- stage output is no longer 45° at the center frequency of the PPF. As the load capacitance increases, the frequency at which the phase difference is 45° gradually decreases.

The load capacitors also affect the fundamental frequency rejection technique. They prevent the complete cancellation of the fundamental tone. The fundamental residue, $S_{residue}$, can be defined as the sum of three signals (V_{1I+}, V_{1Q-}, and V_{2I-}) over V_{in}. This is expressed as

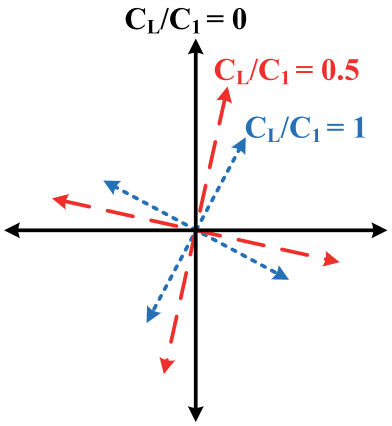

FIGURE 11. Vector diagram of the I/Q signals with load capacitors(C_L).

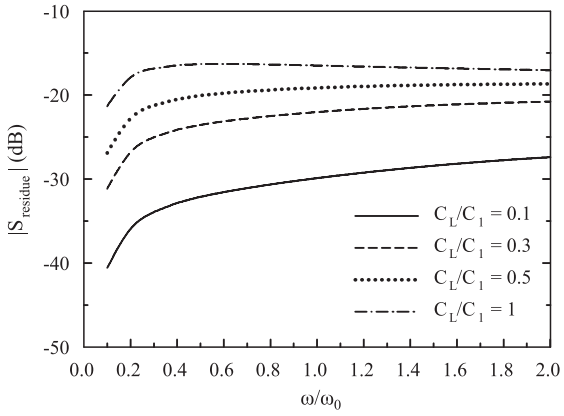

FIGURE 12. Fundamental residue with load capacitors.

follows:

$$S_{residue} = (V_{1I+} + V_{1Q-} + V_{2I-})/V_{in} = \frac{(C_L/C_1)((\omega/\omega_0)^2 + j(\omega/\omega_0))}{A(\omega)} \quad (11)$$

The absolute value of the fundamental residue over the load capacitance is shown in Fig 12. As the load capacitance increases, the fundamental residue also increases. In this work, R_1 and C_1 are 151 ohm and 94.8 fF, respectively. Further, C_L/C_1 is approximately 0.4−0.5. The fundamental residue is < -19.14 dB when $\omega/\omega_0 \leq 1$ and $C_L/C_1 = 0.5$.

B. 3× SUBHARMONIC MIXER

The schematic of the new 3×SHM core is shown in Fig. 13. The proposed 3×SHM core consists of three double-balanced active sub-mixers. If the fundamental signal is balanced, odd-order harmonics remain balanced. Therefore, the 3×SHM shown in Fig. 13 can be regarded as a double-balanced 3×SHM. The differential baseband signal is mixed with each differential LO signal and up-converted to the differential RF signals. These up-converted differential RF signals still maintain the same phase interval as the LO signals. These up-converted current signals are summed at the RF+ and RF−. The fundamental RF signals are finally cancelled and the desired signals mixed with the third-order harmonic of LO are boosted by $2\sqrt{2}$ times as shown in Fig. 2. The size of the transistors and the current consumption of all the sub-mixers are the same owing to the octet-phase generator that can generate $\sqrt{2}$ times boosted and 45° phase-shifted LO signals. The gate width of the transconductance stage (M_1) and switching stage (M_2) are 100 μm and 30 μm, respectively with the gate length of 65 nm.

The fundamental tones ($f_{LO} \pm f_{BB}$) can be suppressed by not only the fundamental frequency rejection technique but also the frequency response of the output load (LC-tank). To verify the fundamental frequency rejection technique, the fundamental tone suppression (1st suppression) of the 3×SHM core is simulated and compared to with and without employing the fundamental frequency rejection technique as shown in Fig. 14. Without the fundamental frequency rejection technique, all the sub-mixers are driven with the same LO phase (0° and 180°). The fundamental tones ($f_{LO} \pm f_{BB}$) are suppressed >24 dBc than the desired tones ($3f_{LO} \pm 3f_{BB}$) at

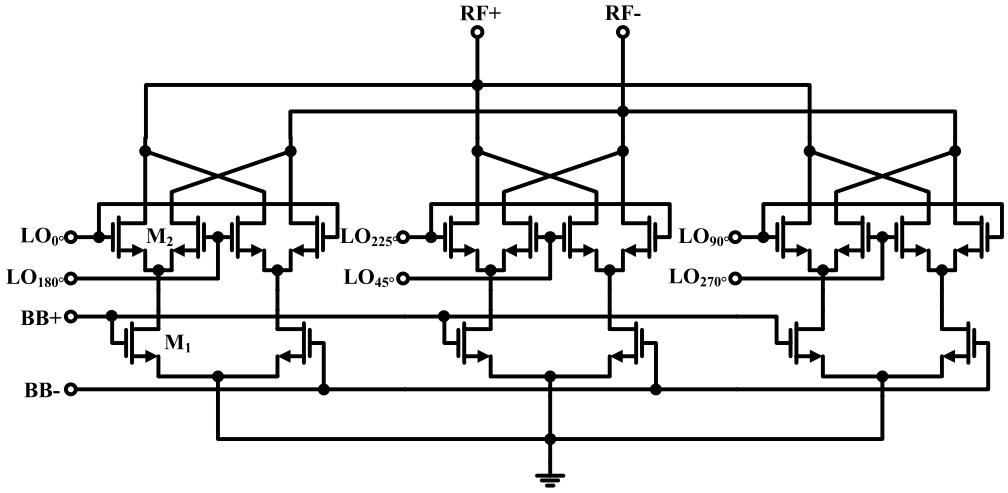

FIGURE 13. Schematic of a 3×SHM core.

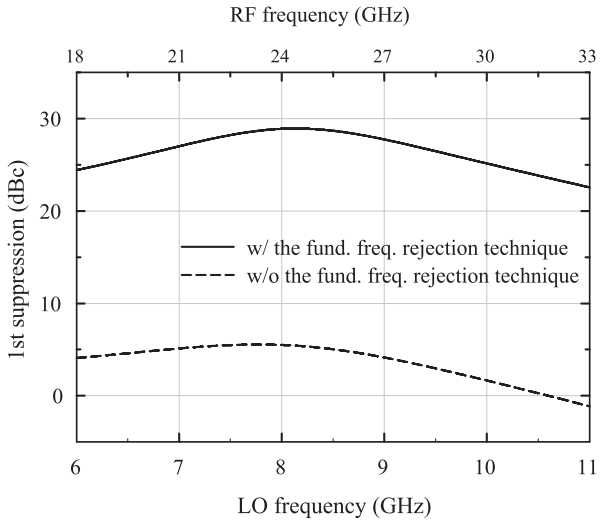

FIGURE 14. Simulation results of fundamental tone suppression.

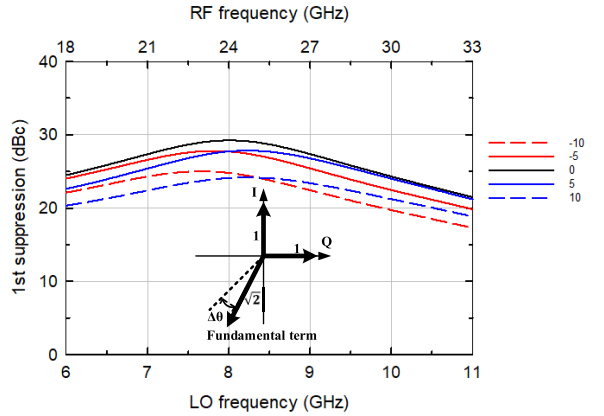

FIGURE 15. Simulation results of mismatch effect of fundamental tone suppression.

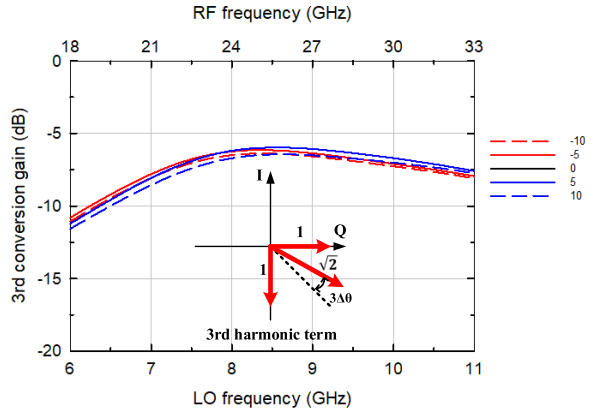

FIGURE 16. Simulation results of mismatch effect of 3rd conversion gain.

19.5−31.5 GHz. Owing to the fundamental frequency rejection technique, the fundamental tone suppression is improved >21 dBc at 19.5−31.5 GHz.

Only the inductor is simulated by EM, and the core connection part is simulated by extracting on the capacitance by parasitic extraction (PEX). Parasitics that were not considered may have affected the suppression. Fig. 15, 16 are the results

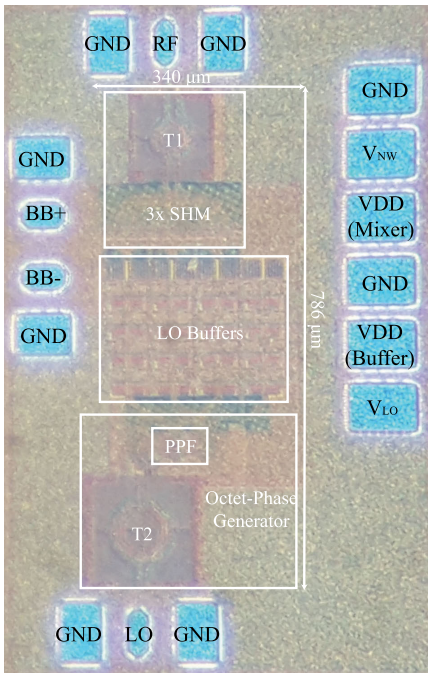

FIGURE 17. Microphotograph of a prototype of the 3×SHM.

of simulating how the suppression effect can be changed due to mismatch that can be caused by these factors. It is suppression due to mismatch of 5° and 10° from the 45° reference of the 8-PG, and system is functional although there is slight gain drop. Even if a phase error of 10° occurs, it can be seen from the trigonometric identities that there is no significant effect on performance.

IV. EXPERIMENTAL RESULTS

The proposed 3×SHM is implemented using a 65 nm CMOS process. A microphotograph of the prototype of the 3×SHM is shown in Fig. 17 and its size is $340 \times 786\ \mu m^2$. V_{LO}, which is the DC voltage of gate of switching stages, is 1 V. V_{NW} is an n-well voltage of deep n-well nMOS transistors and is the same as VDD. At the gates of the transconductance stages (BB+ and BB−), a DC voltage of 0.55 V is applied using the DC offset of the signal generator. The power consumption of the 3×SHM core and LO buffers is 25.2 mW and 30.45 mW, respectively. The number of LO buffers is three times that of the general fundamental mixer owing to the fundamental frequency rejection technique. However, the power consumption of LO buffers may not be a problem, because the operation frequency of the LO buffers is reduced to one-third.

The proposed 3×SHM is measured using a Keysight E4438C ESG vector signal generator, Anritzu MG3694C signal generator, and Anritzu MS2830A signal analyzer. Fig. 18 shows the simulated and measured conversion gains (CG) of the 3×SHM. The simulated and measured conversion gains mixed with $3f_{LO}$ (3rd CG) are −5.0±1.6 and −5.1±1.5, respectively, at 19.5−31.5 GHz and the LO power of 5 dBm. As any other subharmonic mixer the conversion gain is low.

TABLE 2. Comparison table with up-conversion SHMs.

	[18]	[19]	[20]	[21]	[22]	This work
Technology	0.13 μm CMOS	0.15 μm mHEMT	0.15 μm pHEMT	65 nm CMOS	65 nm CMOS	65 nm CMOS
Type	2×SHM	2×SHM	2×SHM	2×SHM	2×SHM	3×SHM
RF Freq. [GHz]	58−66	37.5−42.5	39−41	30−65	36−42	19.5−31.5
3dB−gain BW [GHz]	8	5	2	18	6	12
Conversion Gain [dB]	5	−0.2	−1	−8	5.3±1.2	−5.1±1.5
LO power [dBm]	5	15	9.5	4	5	5
OP_{1dB} [dBm]	−10	−26	−20	−25	−10	−15.4
OIP3 [dBm]	N/A	−10	−5	−18	N/A	−7.6
LO-RF isolation [dB]	>40	>20	>35	N/A	>64	>42
2LO-RF isolation [dB]	>25	>30	>40	>42	>50	N/A
3LO-RF isolation [dB]	N/A	N/A	N/A	N/A	N/A	>46
Power consumption [mW]	92.2	32.2	51.6	21	21.2	55.65
Size [mm^2]	0.366	1.17	1.26	0.498	0.85	0.267

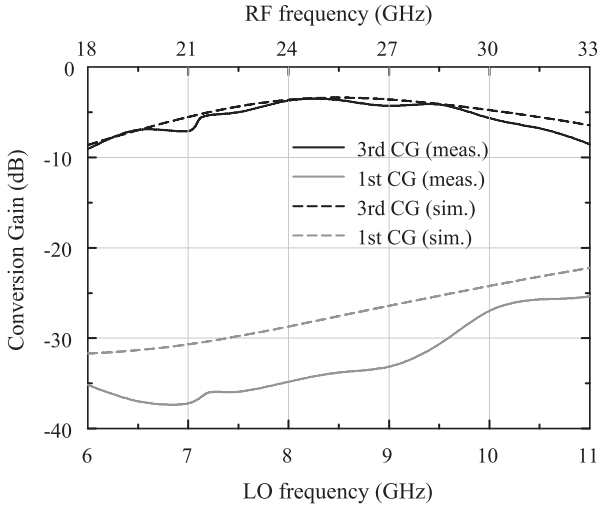

FIGURE 18. Simulated and measured conversion gains of the 3×SHM.

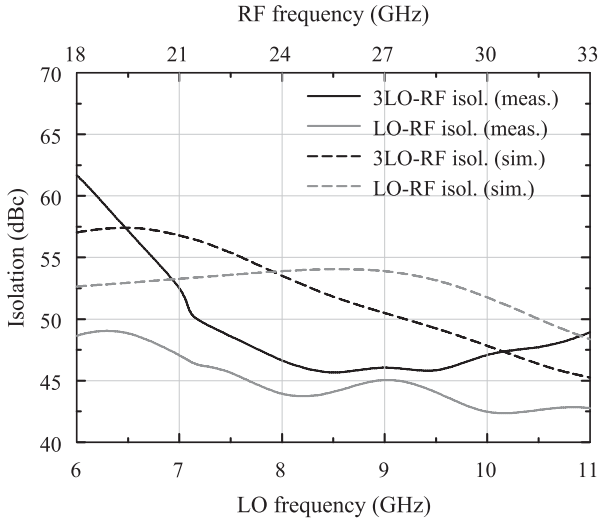

FIGURE 19. Simulated and measured LO-RF isolation and 3LO-RF isolation of the 3× SHM.

Because the mixer is using the nonlinearity of harmonics rather than fundamental. The measured 3-dB gain bandwidth is 12 GHz. The simulated and measured maximum conversion gains are −3.4 dB and −3.6 dB at 25.5 GHz, respectively. The simulated and measured conversion gains mixed with the fundamental LO (1st CG) are from −31.3 to -23.2 dB and from −37.2 to −25.7 dB, respectively, at 6.5−10.5 GHz and the LO power of 5 dBm. The measured fundamental tone is suppressed >30 dBc at the LO of 6.5−8.5 GHz (RF of 19.5−25.5 GHz). The undesired signal mixed with the fundamental LO is well suppressed below the desired RF signal mixed with the third-order harmonic of the LO. The simulated and measured LO-RF isolation and 3LO-RF ($3f_{LO}$ at RF port) isolation are shown in Fig. 19. The simulated LO-RF isolation and 3LO-RF isolation are >50.3 dB and >46.5 dB, respectively. The measured LO-RF isolation and 3LO-RF isolation are >42 dB and >46 dB, respectively. Unlike the simulation results, the measured LO-RF isolation is worse than the 3LO-RF isolation owing to direct coupling of fundamental LO. Due to routing differences between the PPF and the mixer, a phase error created, which particularly worsens the 1st CG. The simulated and measured 1st CG and 3rd CG at the LO power are shown in Fig. 20.

Fig. 21 shows the simulated and measured output power and conversion gain versus input power. The simulated and measured output 1-dB gain compression point(OP_{1dB}) with the BB of 1 MHz is −12.8 dBm and −15.4 dBm at the LO of 8 GHz and RF of 24.001 GHz, respectively. The simulated and measured output third-order intercept points with the two tones of 0.9 MHz and 1.1 MHz are −4.5 dBm and −7.6 dBm, respectively, at the LO of 8 GHz, as shown in Fig. 22. Table 2 summarizes the performance of the proposed 3×SHM mixer and compares it with other

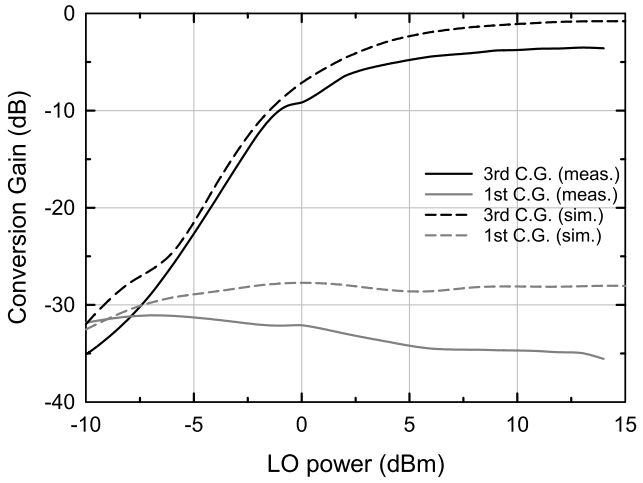

FIGURE 20. Simulated and measured conversion gains at the LO power.

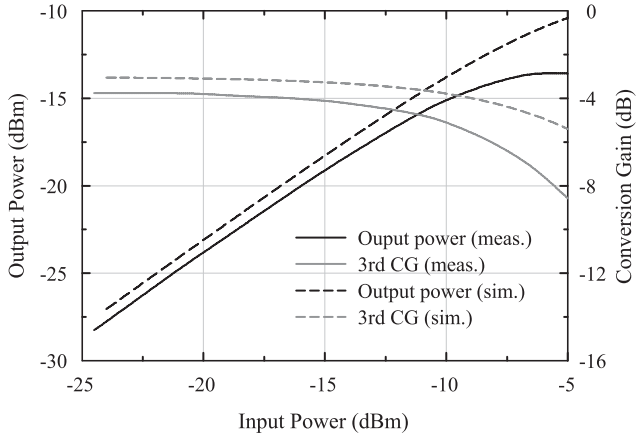

FIGURE 21. Simulated and measured output power and conversion gain at the LO power of 5 dBm.

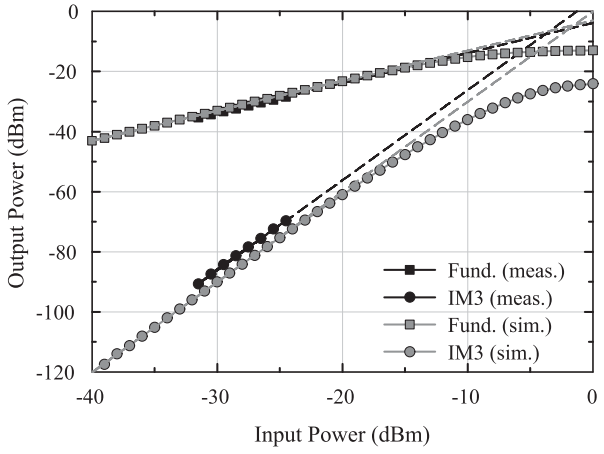

FIGURE 22. Simulated and measured third-order intercept points at the LO power of 5 dBm.

up-conversion 2×SHMs [18]–[22]. The performance of the proposed 3×SHM is similar to that of the other up-conversion 2×SHMs. The proposed up-conversion 3×SHM provides higher 3-dB gain bandwidth, higher isolation, and smaller chip area.

V. CONCLUSION

A new up-conversion 3×SHM mixer designed using a 65 nm CMOS process is presented. The proposed 3×SHM is designed using the fundamental frequency rejection technique to cancel the fundamental LO and boost the third-order harmonic. Three differential LO signals for fundamental frequency rejection technique are generated by an octet-phase generator, which consists of a transformer balun and a two-stage PPF. The 3×SHM core is composed of three Gilbert-cell active sub-mixers to combine three up-converted RF signals and implement the fundamental frequency rejection technique. The measured conversion gain is -5.1 ± 1.5 dB at the RF of 19.5−31.5 GHz and the 3dB-gain bandwidth is 12 GHz. The measured OP_{1dB} and OIP3 are −15.4 dBm and −7.6 dBm, respectively. The LO-RF isolation and 3LO-RF isolation are >42 dB and >46 dB, respectively. The total power consumption of the proposed 3×SHM is 55.65 mW and the 3×SHM occupies a chip area of 0.267 mm^2. The performance of this 3×SHM is similar to that of other up-conversion 2×SHMs.

ACKNOWLEDGMENT

The MPW was supported by IDEC.

REFERENCES

[1] A. Abidi, "Direct-conversion radio transceivers for digital communications," *IEEE J. Solid-State Circuits*, vol. 30, no. 12, pp. 1399–1410, Dec. 1995.

[2] S. Bronckers, A. Roch, and B. Smolders, "Wireless receiver architectures towards 5G: Where are we?" *IEEE Circuits Syst. Mag.*, vol. 17, no. 3, pp. 6–16, 3rd Quart., 2017.

[3] B. Razavi, "RF transmitter architectures and circuits," in *Proc. IEEE Custom Integr. Circuits Conf.*, 1999, p. 197–204.

[4] T. H. Lee and A. Hajimiri, "Oscillator phase noise: A tutorial," *IEEE J. Solid-state Circuits*, vol. 35, no. 3, pp. 326–336, Mar. 2000.

[5] B. R. Jackson and C. E. Saavedra, "A CMOS Ku-band 4x subharmonic mixer," *IEEE J. Solid-State Circuits*, vol. 43, no. 6, pp. 1351–1359, Jun. 2008.

[6] R. M. Kodkani and L. E. Larson, "A 24-GHz CMOS passive subharmonic mixer/downconverter for zero-IF applications," *IEEE Trans. Microw. Theory Techn.*, vol. 56, no. 5, pp. 1247–1256, May 2008.

[7] A. Mazzanti, M. Sosio, M. Repossi, and F. Svelto, "A 24 GHz subharmonic direct conversion receiver in 65 nm CMOS," *IEEE Trans. Circuits Syst. I, Reg. Papers, Reg. Papers*, vol. 58, no. 1, pp. 88–97, Jan. 2011.

[8] K.-J. Koh, M.-Y. Park, C.-S. Kim, and H.-K. Yu, "Subharmonically pumped CMOS frequency conversion (up and down) circuits for 2-GHz WCDMA direct-conversion transceiver," *IEEE J. Solid-State Circuits*, vol. 39, no. 6, pp. 887–884, Jun. 2004.

[9] L. Sheng, J. C. Jensen, and L. E. Larson, "A wide-bandwidth Si/SiGe HBT direct conversion subharmonic mixer/downconverter," *IEEE J. Solid-State Circuits*, vol. 35, no. 9, pp. 1329–1337, Sep. 2000.

[10] T. Yamaji, H. Tanimoto, and H. Kokatsu, "An I/Q active balanced harmonic mixer with IM2 cancellers and a 45° phase shifter," *IEEE J. Solid-State Circuits*, vol. 33, no. 12, pp. 2240–2246, Dec. 1998.

[11] J.-S. Syu, C. C. Meng, and C.-L. Wang, "A 2.4-GHz low-flickernoise CMOS sub-harmonic receiver," *IEEE Trans. Circuits Syst. I, Reg. Papers, Reg. Papers*, vol. 60, no. 2, pp. 437–447, Feb. 2013.

[12] M. Shimozawa, K. Nakajima, H. Ueda, T. Tadokoro, and N. Suematsu, "An even harmonic image rejection mixer using an eight-phase polyphase filter," in *IEEE MTT-S Int. Microw. Symp. Dig.*, Jun. 2008, pp. 1485–1495.

[13] S.-C. Tseng, J.-S. Syu, J.-Y. Su, H.-J. Wei, C. Meng, and G.-W. Huang, "16.4 GHz SiGe BiCMOS sub-harmonic mixer with reactive I/Q generators in RF and LO paths," in *Proc. Asia Pacific Microw. Conf.*, Dec. 2009, pp. 1172–1175.

[14] J. Im, H.-S. Kim, and D. D. Wentzloff, "A 217μW 82dBm IEEE 802.11 Wi-Fi LP-WUR using a 3rd- harmonic passive mixer," in *Proc. IEEE Radio Freq. Integr. Circuits Symp. (RFIC)*, Jun. 2018, p. 172–175.
[15] J. A. Weldon, et al., "A 1.75-GHz highly integrated narrow-band CMOS transmitter with harmonic-rejection mixers," *IEEE J. Solid-State Circuits*, vol. 36, no. 12, pp. 2003–2015, Dec. 2001.
[16] B. Razavi, *RF Microelectronics*, 2nd ed. Englewood Cliffs, NJ, USA: Prentice-Hall, 2011.
[17] J. S. Syu, C. C. Meng, and Y. H. Teng, "Large improvement in image rejection of double-quadrature dual-conversion low-IF architectures," *IEEE Trans. Microw. Theory Techn.*, vol. 58, no. 7, pp. 1703–1712, Jul. 2010.
[18] P. S. Wu, C. H. Wang, C. S. Lin, K. Y. Lin, and H. Wang, "A compact 60 GHz integrated up-converter using miniature transformer couplers with 5 dB conversion gain," *IEEE Microw. Wireless Compon. Lett.*, vol. 18, no. 9, pp. 641–643, Sep. 2008.
[19] J. Y. Su, C. Meng, and P. Y. Wu, "Q-band pHEMT and mHEMT subharmonic Gilbert upconversion mixers," *IEEE Microw. Wireless Compon. Lett.*, vol. 19, no. 6, pp. 392–394, Jun. 2009.
[20] C. C. Meng, J. Y. Su, H. J. Wei, P. Y. Wu, and G. W. Huang, "40-GHz high-linearity single-voltage-supply pHEMT Gilbert sub-harmonic upconverter using leveled-LO topology," in *IEEE MTT-S Int. Microw. Symp. Dig.*, Oct. 2011, pp. 21–24.
[21] P.-H. Tsai, C.-C. Kuo, J.-L. Kuo, S. Aloui, and H. Wang, "A 30×2013;65 GHz reduced-size modulator with low LO power using sub-harmonic pumping in 90-nm CMOS technology," in *Proc. IEEE Radio Freq. Integr. Circuits Symp.*, Jun. 2012, p. 491–494.
[22] H.-H. Lin, Y.-H. Lin, H.-C. Lu, and H. Wang, "A 38-GHz up-conversion sub-harmonic mixer with buffer amplifier in 65-nm CMOS process," in *Proc. IEEE Asia Pacific Microw. Conf. (APMC)*, Nov. 2017, p. 551–553.

HYO-SUNG LEE (Member, IEEE) was born in Seoul, South Korea. He received the B.S. degree in electronic and electrical engineering from Sungkyunkwan University, Suwon, South Korea, in 2011, and the Ph.D. degrees in electrical and electronics engineering from Yonsei University, Seoul, in 2018. He is currently working at Samsung Electronics. His research include microwave and millimeter-wave RFIC and modules for mobile 5G mmWave communications.

JONGHOON MYEONG (Graduate Student Member, IEEE) received the B.S. degree in electronic and electrical engineering from Yonsei University, Seoul, South Korea, in 2016, where he is currently pursuing the Ph.D. degree. His research interests include CMOS RFIC and communication systems for microwave and millimeter-wave applications.

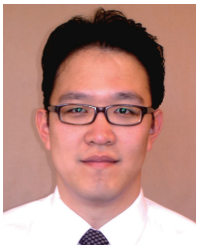

BYUNG-WOOK MIN (Member, IEEE) was born in Seoul, South Korea. He received the B.S. degree from Seoul University, Seoul, in 2002, and the M.S. and Ph.D. degrees in electrical engineering and computer science from the University of Michigan at Ann Arbor, in 2004 and 2007, respectively.

From 2006 to 2007, he was a Visiting Scholar with the University of California at San Diego, La Jolla. From 2008 to 2010, he was a Senior Engineer with Qualcomm Inc., Santa Clara, CA and Austin, TX. He is currently an Associate Professor with the Department of Electrical and Electronic Engineering, Yonsei University, Seoul. His research interests include Si/SiGe RFIC and communication systems for microwave and millimeter-wave applications.